

J. C. Hamer

R. S. Sayles

Department of Mechanical Engineering,
Imperial College,
London SW8 England

E. Ioannides

SKF ERC,
The Netherlands

The Collapse of Sliding Micro-EHL Films by Plastic Extrusion

In the mixed lubrication regime, where surface roughness may exceed the elasto-hydrodynamic film thickness, sliding micro-ehl films appear to collapse during their passage through the contact. A possible explanation for this can be found if the film is treated as a plastic solid. In this work, the collapse velocity is found by simultaneously solving the plastic extrusion equations and the elastic pressure equations for the film trapped between approaching asperities. The velocity of collapse is shown to be very sensitive to the asperity wavelength, slide-roll ratio, and the velocity profile between the sliding asperities.

Introduction

The ability of rolling contacts to operate satisfactorily at low λ ratios, where the surface roughness may greatly exceed the calculated film thickness is well established. Indeed resistance measurements between rolling surfaces under such conditions indicate that the asperities are completely separated by a continuous film. If the fluid is assumed Newtonian this is to be expected as micro-ehl film will always be generated between asperities. However if some sliding is introduced resistance measurements invariably show significant asperity contact, which in real applications will usually cause increased wear and occasionally scuffing.

A mechanism by which the protective asperity films may collapse has been proposed by Jacobson (1987) based on the well established concept of a limiting shear stress in sliding ehl contacts. This limiting shear stress will always act in the direction of the absolute sliding velocity, so if the transverse sliding velocity of a collapsing asperity film is relatively small as compared to the sliding speed in the rolling direction then the shear stress resisting this flow will also be small and can be expressed as

$$\frac{\tau_y}{\tau_l} = f = \left(\frac{v_s^2}{v_s^2 + u_s^2} \right)^{1/2} \quad (1)$$

This means that asperity films may collapse even under relatively small transverse pressure gradients. Consequently it should be possible from a given pressure gradient and shape of film to determine an equilibrium flow velocity under which micro-films may collapse.

Johnson and Higginson (1988) have used narrow bearing theory in applying this same mechanism to an ideal linear viscoplastic lubricant flowing between parallel, rigid surfaces. In their model the shear was assumed to be Newtonian in the central region of the film with the bulk of the sliding occurring

at the walls as plastic shear. At very high pressures and viscosities the Newtonian pressure flow could be neglected.

These results were compared with experiments carried out on disk which had been machined with circumferential roughness. By measuring the electrical resistance between the disk the authors were able to observe the collapse of the film under different sliding speeds. Although quantification of actual film thickness was difficult, the experiments clearly showed a reduction in thickness of the micro-ehl film at the asperity crests under sliding.

Asperity Collapse in EHL Contacts

In this work an attempt will be made to extend this failure mechanism to real ehl contacts where the asperity pressure distribution is largely determined by the elastic deflections.

Rolling bearing elements are normally circumferentially ground. This leads to a highly anisotropic surface where the wavelength characteristic (β^*) is very much greater in the circumferential direction than in the axial direction. Analysis of such surfaces can be much simplified if each surface is assumed to be two dimensional. The idealized surface then takes a corrugated form which runs continuously around the rolling element circumference.

If the operating conditions are good enough, a thick ehl film will be generated and the asperities will only cause very small perturbations in the macro-ehl pressure distribution. As conditions become poorer the surfaces move closer to one another leading to significant elastic deformation of the asperities and the formation of micro-ehl films. In order to tackle the collapse mechanism of these films it is necessary to estimate their initial thickness.

At severe degrees of interpenetration when the pressures in the valleys surrounding the asperities are low a quite reasonable estimate of the micro-ehl film thickness can be made by simply extending the Dowson and Hamrock film thickness formula (1981) to individual asperities. Films calculated on this basis yield film thickness within 15 percent of those calculated by Snidle et al. (1987) using a full numerical micro-ehl analysis.

The collapse analysis can be further simplified if the micro-

Contributed by the Tribology Division of THE AMERICAN SOCIETY OF MECHANICAL ENGINEERS and presented at the Joint ASME/STLE Tribology Conference, Toronto, Canada, October 7-10. Manuscript received by the Tribology Division March 26, 1990; revised manuscript received July 2, 1990. Paper No. 90-Trib-47. Associate Editor: T. Larsen-Basse.

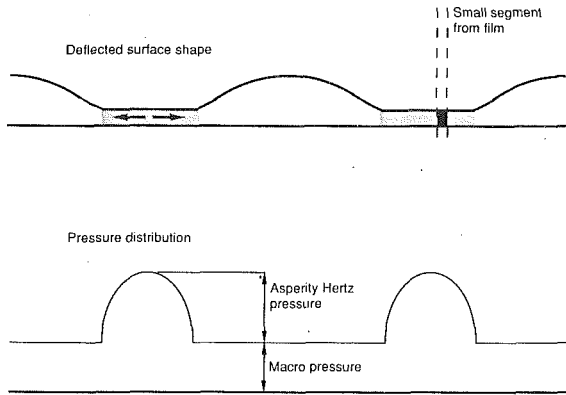


Fig. 1 Cross section through the idealized contacting surface

ehl contact width is assumed constant in its passage through the main ehl zone. As the asperity must enter and leave the contact this is obviously untrue, but the degree of error will depend on the macro-ehl pressures within the contact. If the loads are light or the roughness amplitude is very high, then the micro-ehl contacts may be expected to carry the majority of the load. The pressure distribution will then resemble the dry contact case of a series of elongated ellipses under each circumferential asperity. However if the load is high and the oil assumed incompressible the asperities will undergo some initial flattening in the inlet then continue through the contact with little further deformation as the increasing load is spread across the contact. As the oil film is not incompressible a greater normal approach can be expected between the valleys under higher loads, but the asperity contact patches might still be expected to more closely resemble thin strips with rounded edges than ellipses.

This micro-film may then be treated as a plastic solid which will be extruded out sideways by the pressure gradient existing across the deformed asperity. Unfortunately the rate at which film extrusion occurs is dependent upon the velocity profile through the film thickness. This in turn will depend upon the rheology of the lubricant which at extremely high pressures is unclear. In the narrow bearing analysis of Johnson and Higginson (1988), the slip was assumed to occur at each wall, whereas other workers such as Trachman (1976) have argued that the majority of the slip occurs at the central plane. In thick ehl contacts the latter seems more likely. The conductivity of oil films is poor and temperature differences of the order of 30°C can easily exist between the center and walls of the film. As the limiting shear strength of films reduce with increasing temperature, the resistance to sliding will be minimized if the slip plane occurs in the center of the film.

However micro-ehl films are often only a fraction of the

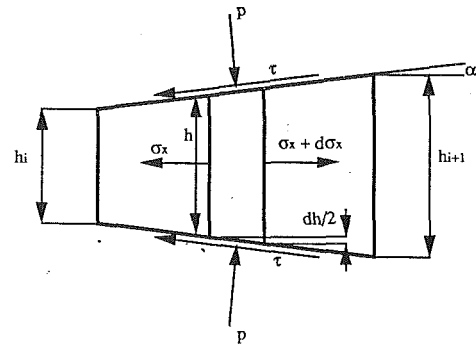


Fig. 2 Small segment from extruding film

thickness of macro-films so the temperature differences are much smaller and the precise location of slip plane or planes is difficult to ascertain. In fact if the shear stress is at all related to the shear rate then the slip might be expected to be more evenly spread across the film.

In Appendix 1 the extrusion velocity is derived in terms of a generalized sliding velocity profile. The trends from this show the collapse velocity to be enhanced as the bulk of the shear is shifted toward the walls. This means that if the slip is divided equally between each film-wall interface then the asperity collapse rate will be maximized (the case used by Johnson and Higginson, 1988). Conversely if the slip plane is formed only on the center plane of the film then sliding in the rolling direction will not enhance the asperity collapse rate at all. Perhaps more realistically if the shear strain rate is assumed roughly constant across the micro-film then asperity collapse rate will be one third of the maximum. In this analysis the film shear is assumed to be shared equally at each wall-film interface. However the results may be easily modified to suit different velocity profiles by means of the factors discussed above.

Theoretical Model

A cross section through the idealized contacting surface is shown schematically in Fig. 1.

Each extruding micro-film can be divided into a series of small segments, Fig. 2. Although the film will probably begin near parallel, during collapse each segment may take up some slope α . A normal pressure and tangential shear stress will act on the top and bottom of a small element of the segment and a resultant force due to the pressure gradient will act on each side. Resolving these forces in the y direction

$$\sigma_x dh + h d\sigma_x + p dh - \tau \cot(\alpha) dh = 0 \quad (2)$$

For small values of α , $p \gg \tau$, so p and σ_x may be considered as principal stresses. According to the Von Mises yield criterion

Nomenclature

d = length of segment, (m)	s = separation of undeflected surfaces, (m)	z = coordinate in direction of velocity; w
d_0 = amplitude of undeformed asperity, (m)	t' = time interval, s	α = half angle between deflected surfaces
f = shear stress reduction factor	u = velocity in rolling direction, (m/s)	β = distance over which correlation length decays to $1/e$
h = film thickness, (m)	v = velocity in axial direction, (m/s)	γ = shear strain rate, 1/s
i, j = intervals	w = velocity through film thickness, (m/s)	σ = normal stress, (Pa)
k = yield shear stress, (Pa)	x = coordinate in direction of velocity; u	
l = asperity wavelength, (m)	y = coordinate in direction of velocity; v	
n = number of intervals		
p = film pressure, (Pa)		
p_{asp} = asperity pressure, (Pa)		
p_{HZ} = macro-hertz pressure, (Pa)		
q = plastic flow rate, m^2/s		

Subscripts

o = end of segment
s = sliding

in plane strain, the difference in principal stress will equal twice the uniaxial yield shear stress k , thus

$$\sigma_x + p = 2k \quad (3)$$

For an oil film in the glassy state the traction coefficient (μ) which effectively is k/p is constant, so:

$$k = \mu p \quad (4)$$

Substituting into equation (3)

$$\sigma_x = (2\mu - 1)p \text{ and } d\sigma_x = (2\mu - 1)dp \quad (5)$$

The shear stress at the film/roller surface interface in the lateral flow direction will equal k times the shear stress reduction factor f , (equation (1)). So:

$$\tau = f\mu p \quad (6)$$

Equation (2) becomes,

$$\mu(2 - f)\cot(\alpha)pdh = h(1 - 2\mu)dp \quad (7)$$

and integrating,

$$\ln(p) = \frac{\mu(2 - f)\cot(\alpha)}{(1 - 2\mu)} \ln(h) + \text{const} \quad (8)$$

Then by dividing the film into small segments of length, d , the pressure and height at each end of a segment can be related to the shear stress reduction factor as

$$f = \left(\frac{\ln\left(\frac{p}{p_0}\right)(2\mu - 1)}{\ln\left(\frac{h}{h_0}\right)\mu} + 2 \right) \left(\frac{h - h_0}{d} \right) \quad (9)$$

In order that Dowson and Hamrock's film thickness formula may be applied to micro-ehl, each asperity peak and valley is assumed to have a constant radius of curvature. If the angle of arc is fairly small the shape of each arc can be expressed as a parabola

$$s = \frac{(l^2 - 4y^2)}{8R} \quad (10)$$

The undeflected gap can be described as

$$s = \frac{2d_0(l^2 - 4y^2)}{l^2} \text{ for } y = 0 \text{ to } \pm \frac{l}{2} \quad (11)$$

$$s = \frac{2d_0(l^2 - 4(l - |y|)^2)}{l^2} \text{ for } y = \frac{l}{2} \text{ to } \pm l \quad (12)$$

The initial micro-ehl film thickness under each asperity has been calculated using conventional ehl theory. Therefore the film thickness may be assumed to be initially near constant under each deflected asperity. As the asperities have a constant radius of curvature the pressure distribution may be described as a micro-hertz pressure distribution (for an asperity of radius, R) superimposed upon the average macro-ehl pressure across the contact (Fig. 1). This can be expressed as

$$p = p_{\text{HZ}} + p_{\text{asp}} \left(1 - \frac{y^2}{a_{\text{asp}}^2} \right)^{0.5} \text{ for } |y| = 0 \text{ to } a_{\text{asp}} \quad (13)$$

$$p = p_{\text{HZ}} \text{ for } |y| > a_{\text{asp}} \quad (14)$$

Therefore from the height and pressure at each end of a segment and the appropriate shear stress reduction factor f , the sliding velocity ratio can be derived from equation (9). The extrusion velocity v_e can be expressed as q_i/h_i where q_i is the plastic flow rate through the segment.

Therefore from equation (1);

$$q_i = \frac{h_i \mu_s f}{(1 - f^2)^{1/2}} \quad (15)$$

Each segment will have to rise or fall in order to maintain

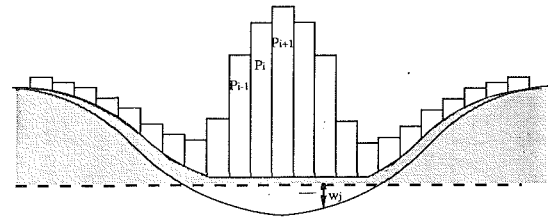


Fig 3 Schematic diagram of pressure distribution and deflected shape

continuity of flow. If each segment collapses at velocity w_i , then

$$w_i = \frac{(q_i - q_{i-1})}{d} \quad (16)$$

As the asperity collapses the shape of the gap will change and so will the pressure distribution and consequently the flow rate. Accordingly the calculated flow rates are assumed constant for small time intervals t' , after which a new set of film thicknesses (h'_i) can be found at each segment;

$$h'_i = h_{(\text{initial})i} - t'w_i \quad (17)$$

As the asperity is symmetric these heights can be reflected around the centerline to determine the new asperity shape over one complete wavelength. By subtracting this new shape from the undeformed asperity profile, the new elastic deflection at each interval can be found.

Although the undeformed surface profile is two dimensional the deformed asperity shape and pressure distribution will vary in both the transverse and rolling direction. However as the radii of curvature of the asperities is very much less than that of the rolling element, the pressure gradients and slopes in the transverse direction are very much greater than in the rolling direction. It is perhaps not unreasonable then to use a two-dimensional plane strain approach and assume the pressure distribution is constant in the rolling direction. As determination of the elastic pressure involves matrix inversion this 2-D simplification represents a very large saving in computing time.

In a line loading of a semi-infinite halfspace the strains are proportional to $1/r$, so the displacements, proportional to $\ln(r)$, will always remain infinite and thus have to be calculated relative to some datum point. In this problem the asperities are symmetric and identical so as each asperity collapses there will be no net flow between adjacent asperities. This datum can then be conveniently placed at $h(\text{max})$. This will clearly not exactly satisfy the condition that the total oil volume and load carried within each asperity wavelength must remain constant. However as the fraction of the film under the asperity is very small and its thickness is much less than the elastic deflection, the collapse of the film is unlikely to significantly alter the bulk macro-conditions. The entire wavelength can be divided into N intervals which are coincident with each of the segments of the plastic extrusion and over which the pressure is assumed uniform (Fig. 3). The general deflection at each interval, i due to the unit pressure interval, j can be related by a matrix of influence coefficients C_{ij} as follows

$$W_i = \frac{-d}{2\pi E^*} \sum C_{ij} p_j \quad (18)$$

For uniform pressure elements in plane strain, the influence coefficients can be written as

$$C_{ij} = [(2|i - j| + 1)\ln(2|i - j| + 1)^2 - (2|i - j| - 1)\ln(2|i - j| - 1)^2] - [(2|n - j| + 1)\ln(2|n - j| + 1)^2 - (2|n - j| - 1)\ln(2|n - j| - 1)^2] \quad (19)$$

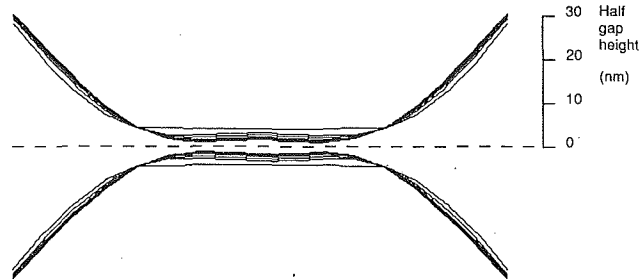


Fig. 4 Cross section of collapsing asperity film shape at 10 micro-second intervals

The pressure deflection relationship can now be expressed as a system of n simultaneous linear equations which are solved numerically.

This new set of pressure elements can be combined with the deflected shape in the extrusion equations to produce a new set of flow rates. As before, the continuity of flow condition can then be applied to determine a new set of segment collapse velocities and thus a new collapsed film shape after time interval t' . This loop is repeated until an equilibrium film shape is reached for the initial time interval. This film shape then provides a new set of $h_{(initial)}$ values and the whole iterative procedure is repeated for the next time interval. Using this technique the collapsing film shape can be found and the velocity at which it collapses.

The objective of the solution is to find a solution which satisfies both the plastic extrusion and elasticity equations. Some of the problems encountered are similar to those arising in traditional ehl solutions which require the simultaneous solution of the Reynolds and elasticity equations. The main difficulty is the high sensitivity of the shape of the relatively thin film shape to small changes in elastic pressure. Deriving the elastic deflections directly from the extrusion pressures was unsuccessful. Although efficient in terms of computing time this proved impossible to converge and the more time consuming matrix inversion method had to be utilized instead. Even so relatively small time steps were necessary to achieve convergence.

Results

These results were computed assuming the asperity width remains substantially constant throughout the contact. First, the collapsing shape and approach velocity of a typical longitudinal asperity will be considered. The selected asperity is representative of a ground bearing surface operating in a bearing under 50 percent sliding. The geometric and dynamic parameters are as follows.

Wavelength	20 micron
Amplitude	0.1 micron
Sliding speed	2 m/s
Rolling speed	5 m/s
Traction coefficient	0.04
Mean film thickness	0.2 micron
Initial asperity film thickness	0.01 micron
Contact width	0.5 mm

In Fig. 4, a cross section of the asperity is shown after 10 μ s time intervals. The rate of asperity film collapse decreases as the film becomes thinner. This is of course to be expected, as the extruding force hdp/dy decreases with the film thickness so must the shear stress resisting the flow. Therefore the extruding velocity (v_x) component of the sliding velocity must also reduce proportionately.

The initial rate of collapse is smallest in the center and increases to a maximum near to each edge of the asperity contact. As collapse continues these differences diminish until

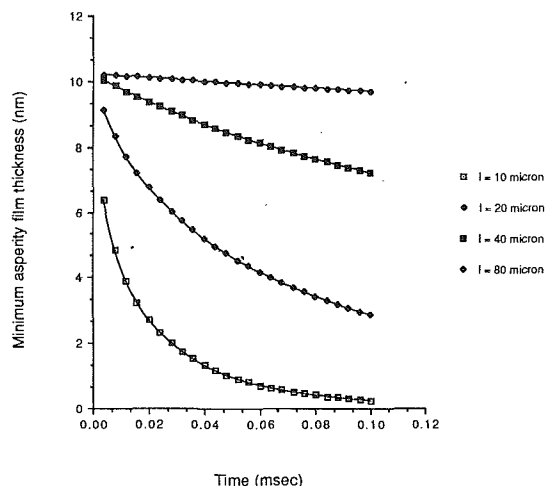


Fig. 5 Plot of minimum film thickness during collapse for different asperity wavelengths

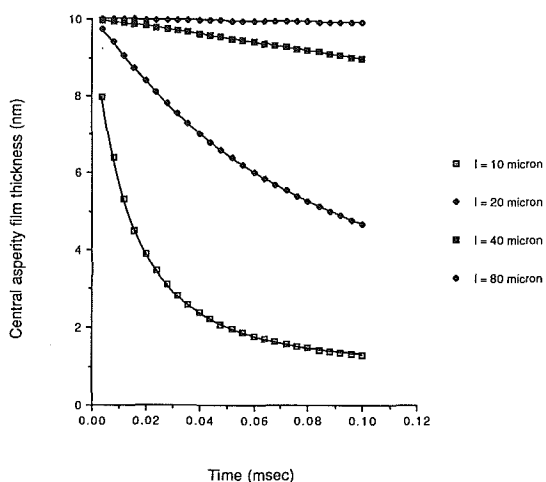


Fig. 6 Plot of central film thickness during collapse for different asperity wavelengths

a near steady state shape is reached. In explaining this behavior it is necessary to consider the changing pressure distribution. Initially this is Hertzian, so the extrusion force, proportional to the pressure gradient will be zero in the center of the contact and increase towards the periphery. The flow rate at any point, will be proportional to the integral of the collapse velocity between that point and the center point. Assuming, therefore that the collapse velocity always remains positive the extrusion velocity and consequently the shear stress resisting the flow must increase between the center and periphery of the contact. As collapse continues a balance has to be reached between the pressure gradient and film thickness, which define the extrusion force, the normal pressure and flow velocity.

In Figs. 5 and 6 the minimum and central film thicknesses are plotted against time for different values of wavelength. The asperity amplitude remains unaltered so the average macro-ehl film thickness remains reasonably constant. With increasing wavelength the extrusion path length increases and the pressure gradient decreases, so the collapse rate diminishes rapidly. This effect combined with an initially thicker micro-film means that the risk of micro-ehl collapse may be significantly reduced if a longer wavelength surface structure can be produced.

In Fig. 7 the relationship between minimum film thickness and rolling speed for different slide-roll ratios is shown. The shear stress in the y direction is proportional to the transverse

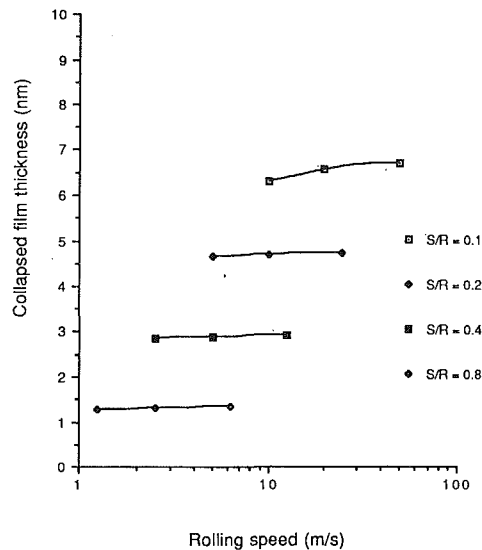


Fig. 7 Plot of relationship between minimum film thickness and rolling speed for different slide-roll ratios

sliding velocity divided by the rolling direction sliding velocity, so clearly if the sliding velocity increases, the extrusion velocity will also increase to maintain the same y direction shear stress. However as rolling speed is increased the contact duration reduces. The net effect of this is that film collapse is fairly insensitive to rolling speed, but is very dependent upon the slide-roll ratio.

Finally the effect of traction coefficient on the minimum film thickness is shown in Fig. 8. For a given set of operating conditions increasing the traction coefficient will just increase the film resistance to extrusion so the collapse rate will reduce. Of course an oil having a higher traction coefficient may have very different rheological properties with respect to the sliding velocity profile which are not possible to predict in this analysis.

Conclusions

The limiting shear stress concept applied to a plastic film, provides a powerful mechanism in explaining the collapse of asperity separating films under rolling/sliding conditions. When applied to ehl contacts the mechanism of collapse shares similarities with the squeeze film formed between normally approaching cylindrical contacts where a dimple is generated in the center of the contact which then collapses. The results of this micro-elastic study reinforce the results of earlier workers (Jacobson et al. (1987) and Johnson and Higginson (1988)), although the collapse velocities are a little lower. As expected, reducing the asperity wavelength or increasing the sliding speed, increases the likelihood of film collapse. Although increasing the traction coefficient reduces the collapse rate this must be offset by the increased shear heating which will reduce the initial film thickness.

The mechanism of film collapse can be seen to be very dependent on the velocity profile across the sliding film. The authors laboratory has made several attempts to measure this experimentally but so far has had little success. This appears to be a very difficult measurement to achieve experimentally, and to our knowledge has not yet been performed elsewhere. The work reported here shows the film collapse based on a linear shear profile which in turn defines a parabolic extrusion velocity profile. In practical terms, such an assumption must be assumed as somewhat simplistic. The scale of size involved means that treating the film as homogeneous particularly if E. P. or other additives are present, may be unrealistic. However this in itself serves to demonstrate that this area of research needs much work, particularly as the location of the sliding

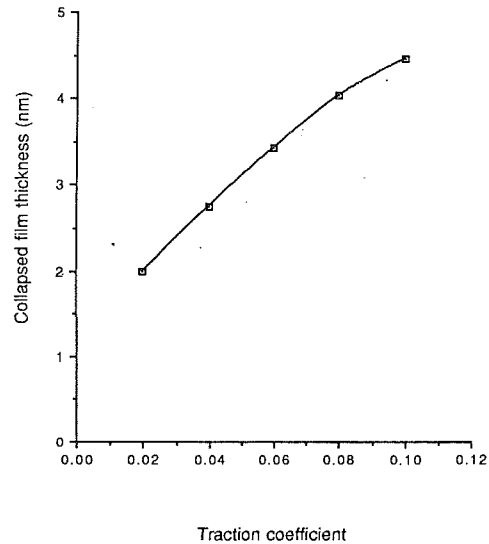


Fig. 8 Plot of relationship between minimum film thickness and traction coefficient

planes and the value of traction coefficient seem to have important roles to play in reducing the risk of scuffing.

Acknowledgments

The authors would like to thank Dr. H. H. Wittmeyer, Managing Director of SKF Engineering and Research Center, for permission to publish this work.

References

- Hamrock, B. J., and Dowson, D., 1981, *Ball Bearing Lubrication*, Wiley.
- Jacobson, B., Ioannides, E., and Tripp, J., 1987, "Redistribution of Solidified Films in Rough Hertzian Contacts," *14th Leeds-Lyon Symposium on Tribology*, Elsevier.
- Johnson, K. L., and Higginson, J. G., 1988, "A Non-Newtonian Effect of Sliding in Micro-EHL," *Wear*, Vol. 128, pp. 249-264.
- Karami, G., Evans, H. P. and Snidle, R. W., 1987, "Elastohydrodynamic Lubrication of Circumferentially Finished Rollers Having Sinusoidal Roughness," *Proc. Inst. Mech. Eng.*, Vol. 201.
- Trachman, E. G., 1976, "A Simplified Technique for Predicting Traction in Elastohydrodynamic Contacts," *ASLE Transactions*, Vol. 21, No. 1, pp. 53-62.

APPENDIX 1

At present the rheological properties of the oil film at extreme pressures are not well understood. Most experimental evidence would suggest that the film reaches a limiting shear stress at a relatively low sliding speed and this limiting shear stress then decreases with increasing sliding speed (shear strain rate). This is in contrast with a classical Bingham Plastic in which the shear stress increases with increasing shear strain rate. However the true isothermal behavior of the film is often obscured by the effects on the rheology of the high temperatures generated in the sliding contact.

If the film behaved as an ideal Bingham plastic the velocity distribution would be near constant through the film thickness. However if as seems likely the yield stress is very sensitive to temperature the velocity gradient will be much steeper near the hot center of the contact. Conversely if the bearing surface/film interface is weak all sliding may take place at the walls. It would be useful therefore to find a general expression for the extrusion velocity in terms of a given sliding velocity profile.

Consider a general continuous velocity distribution across the film in which the velocity gradient is reflected around the centerline. A small plug of the film which is being sheared under sliding in the x and y directions is shown in Fig. A1. If

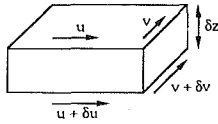
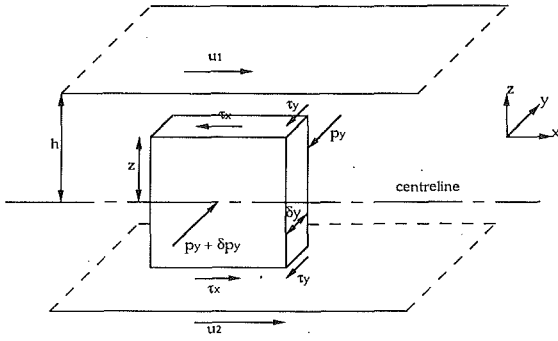


Fig. 1A A small plug of film which is being sheared in both x and y directions

the sliding speed is high relative to the transverse motion then the shear stresses τ_x and τ_y acting on the top and bottom surfaces may be expressed as

$$\tau_x \approx \tau_L \text{ and } \tau_y = z \frac{\partial p}{\partial y} \quad (\text{A1})$$

Across a thin element above the plug there will be a velocity gradient which can be split into components in the x and y direction.

The limiting shear stress will act in the direction of the maximum shear strain rate. Therefore the ratio of the orthogonal shear stresses will equal the ratio of the shear strain rates.

$$\frac{\tau_y}{\tau_x} = \frac{\dot{\gamma}_y}{\dot{\gamma}_x} = \frac{\left(\frac{\partial v}{\partial z}\right)}{\left(\frac{\partial u}{\partial z}\right)} = \frac{\partial v}{\partial u} \quad (\text{A2})$$

Combining equations (A1) and (A2) and

$$\frac{dv}{du} = \frac{z}{\tau_L} \frac{\partial p}{\partial y} \quad (\text{A3})$$

and integrating by parts gives the velocity profile.

$$v = \frac{1}{\tau_L} \frac{\partial p}{\partial y} \int z \cdot du dz \quad (\text{A4})$$

$$v = \frac{1}{\tau_L} \frac{\partial p}{\partial y} \left[z \cdot u - \int u dz \right] \quad (\text{A5})$$

The mean velocity can then be expressed as

$$v_m = \frac{2}{h} \int_0^{\frac{h}{2}} v dz \quad (\text{A6})$$

Consider the case of a constant velocity gradient across the film.

$$u = \frac{(u_1 - u_2)z}{h} \quad (\text{A7})$$

From equation (A5) the velocity profile in the y direction will be

$$v = \frac{(u_1 - u_2)z^2}{2h} + C \quad (\text{A8})$$

At each surface-film interface, $z = h/2$ and $v = 0$, so

$$C = \frac{\partial p}{\partial y} \frac{(u_1 - u_2)h^2}{8h\tau_L} \text{ and } v = \frac{\partial p}{\partial y} \frac{(u_1 - u_2)(3z^2 - h^2)}{8h\tau_L} \quad (\text{A9})$$

This is a parabolic velocity distribution. The mean velocity can then be calculated from equation (A6)

$$v_m = \frac{\partial p}{\partial y} \frac{(u_1 - u_2)}{8h\tau_L} \frac{2}{h} \int_0^{\frac{h}{2}} (3z^2 - h^2) dz \quad (\text{A10})$$

$$v_m = \frac{\partial p}{\partial y} \frac{h(u_1 - u_2)}{12\tau_L} \quad (\text{A11})$$

The calculated mean velocity is one third of that if the film was shearing at each rolling element surface. It appears that the asperities will collapse more rapidly if the velocity gradient is steeper near the walls and more shallow near the centerline. The highest collapse rate will result if the slip is shared equally between the two film/surface interfaces.